Responses to Referee #3's comments

We are grateful to the reviewers for their valuable and helpful comments on our manuscript "**Molecular-level study on the role of methanesulfonic acid in iodine oxoacids nucleation**" (MS No.: egusphere-2023-2084). We have revised the manuscript carefully according to reviewers' comments. The point-to-point responses to the Referee #3's comments are summarized below:

Referee comments:

This manuscript investigates the enhancement effects of methanesulfonic acid (MSA) on the iodic acid (HIO_3)-iodous acid (HIO_2) nucleation system, which has been reported as an important mechanism of marine new particle formation (NPF). The intermolecular interactions, cluster stability, the formation pathway/ free energy surface of cluster formation as well as the enhancement of formation rate of the HIO_3-HIO_2-MSA ternary nucleation system was systematically studied with the combination of quantum chemical simulation and ACDC approach. This paper provided theoretical evidence that the involvement of MSA can structurally stabilize HIO_3-HIO_2-based clusters and has positive synergistic effect on the nucleation with HIO_3 and HIO_2. This manuscript is nicely written and fits the scope of ACP. I recommend the manuscript to be published after the following comments are addressed.

Response: We sincerely thank for the reviewer's careful review of our manuscript, as well as the valuable and positive comments.

General comments:

Comment 1: Although sufficient theoretical details of the cluster conformations have been provided, the authors should also clarify the definition of "stable cluster". We should derive a cluster's concentration by the competition between its collisional formation and evaporation, instead of only judging the formation free energy. Since the authors have conducted ACDC calculations, the evaporation rates of the major clusters should be discussed, as well as the time dependent concentration variations of these major clusters.

Response: Thanks for the reviewer's professional suggestions. Accordingly, we have added the definition of "stable cluster", which is determined based on the competition between cluster

collisional formation and evaporation. A cluster is deemed stable when its collisional formation dominates over evaporation[1]. And the corresponding definition has been added in the revised manuscript (Lines 102-103, page 4) as follows: "Additionally, whether the clusters in the simulated system are stable depends on whether the rate of collision frequencies exceeds the total evaporation rate coefficients ($\beta C/\Sigma\gamma > 1$) (Table S4)."

According to the helpful suggestion of the reviewer, the evaporation rates of the major clusters have been discussed in Lines 175-178 of page 7 as follows: "Generally, stable clusters have lower evaporation rates. According to the calculated cluster evaporation rates ($\Sigma\gamma$, s^{-1}) at 278 K (Table S7), more than 40% of the clusters have $\Sigma\gamma$ less than 10^{-3} s^{-1}, indicating relatively high stability ($\beta C/\Sigma\gamma > 1$). Among these resulting stable clusters (see Fig. S6), the majority (85%) contains HIO_2."

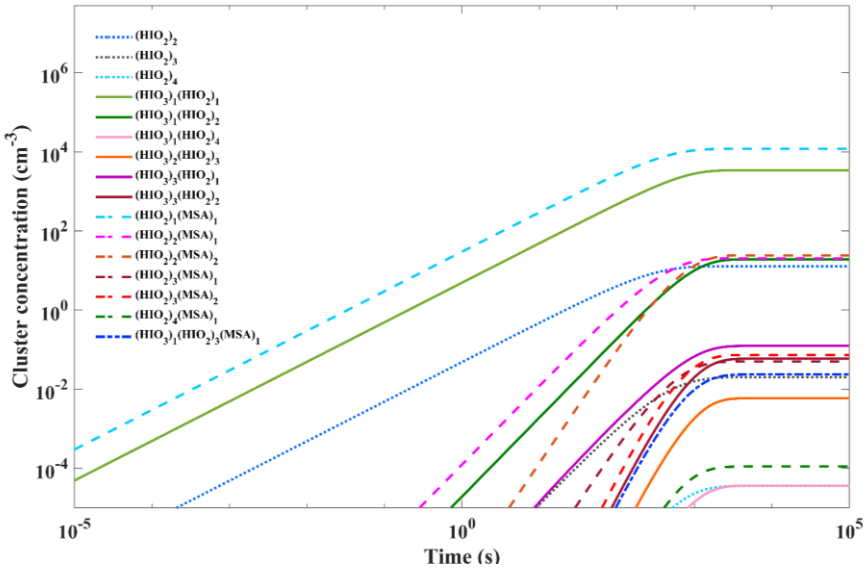

Figure S6. The concentration (molec. cm^{-3}) of stable clusters in HIO_3-HIO_2-MSA system as a function of time, at T = 278 K, CS = 2.0×10^{-3} s^{-1}, [HIO_3] = 10^6, [HIO_2] = 2.0×10^4, [MSA] = 5.0×10^6 molec. cm^{-3}.

Further, as suggested by the reviewer, we calculated the time-dependent concentration variations of the mentioned major cluster sites and presented the simulation results in Fig. S6. The corresponding analysis has been included in the revised manuscript (Line 178-183, page 7), and a copy is provided below: "Moreover, the concentration of these stable clusters increases gradually with time, even reaching a maximum of 10^4 molec. cm^{-3} (Fig. S6). Of these stable clusters, initial $(HIO_3)_1(HIO_2)_1$, $(HIO_2)_2$, and $(MSA)_1(HIO_2)_1$ dimer form rapidly, and at t = ~1

s, heterotrimers $(HIO_3)_1(HIO_2)_2$ and $(MSA)_1(HIO_2)_2$ begin to form, after which, the larger-sized clusters also form. These time-dependent evidence suggests that MSA is involved in the whole clustering process, from the initial formation of smaller clusters to the large-sized nucleated clusters that potentially further grow."

Comment 2: I find the results in section 3.2 a bit confusing when trying to interpret the relative importance of the MSA-involved path in HIO_3-HIO_2-MSA nucleation under different conditions. For example, Figure 3a (upper panel) shows that the MSA-involved path contributes to 74 % of the cluster formation, under [MSA] of 5.0×10^6 molec. cm^{-3}, [HIO_3] of 1.0×10^6 molec. cm^{-3}, while the MSA-involved path contributes to ~20 % under [MSA] of 1.0×10^6 molec. cm^{-3}, [HIO_3] of 1.0×10^6 molec. cm^{-3}. This result indicates that MSA is less efficient in clustering with HIO_2, comparing with HIO_3. The authors have mentioned the atmospheric concentration level of MSA in line 40, the authors should also include the discussion about the concentration of iodine oxoacids in the revised manuscript. Since if the concentration of HIO_3 is comparable or higher than MSA, the scenario of ACDC simulation cannot reflect the condition of real atmosphere.

Response: Thanks for the reviewer's insightful comments. As analyzed by the reviewer, MSA exhibits lower efficiency in clustering with HIO_2 compared to HIO_3. Thus, we agree with the reviewer's suggestion to discuss the conditions with varying iodine oxoacids concentration, as it is very necessary. According to the scenarios presented in Fig. 3(a) (right panel) and Fig. 5 where [HIO_3] is comparable or higher than [MSA], the corresponding analyses were supplemented in the revised manuscript (Line 227-231) and copied below: "However, the atmospheric [HIO_3] ranges widely from 10^6 to 10^8 molec. cm^{-3}. When [HIO_3] is comparable or higher than [MSA], the HIO_3-HIO_2 pathway contributes more, and the *R* of MSA decreases with the rising [HIO_3]. It is worth noting that when [HIO_3] is comparable to [MSA], the *R* of MSA is greater than 2, as the contribution of MSA to clustering includes not only the direct formation of HIO_3-HIO_2-MSA clusters (~20%), but also its 'catalysis' role in facilitating formation of initial HIO_3-HIO_2 clusters (Fig. S7)."

Comment 3: The comparison with field measurements seems to be a bit arbitrary. What's the atmospheric condition such as precursor concentration and temperature of the measurement sites reported? What's the definition of the *J* in the reported field measurements? Can the reported *J* be directly compared with the ACDC simulated *J*? Moreover, in Line 222, "the observed *J* of 2.1 × 10^{-4} cm^{-3} s^{-1}". This *J* value is too low for a typical NPF event. Is this value obtained from a non-NPF day? Please check the original paper. More explanation and discussion are needed in this section, which can sharpen the significance of the theoretical study on the merit of atmospheric implication.

Response: Thanks for the reviewer's professional comments.

Item 1) from the reviewer: The comparison with field measurements seems to be a bit arbitrary. What's the atmospheric condition such as precursor concentration and temperature of the measurement sites reported?

Response: (a) Ny-Ålesund: According to Beck[2] et al., Ny-Ålesund is surrounded by open waters throughout the whole year, with the average annual temperature of -5℃ [3]. As shown in Figure 1(b) of Beck et al., the ranges of [HIO_3] and [MSA] are 10^5 – 10^6 and 10^6 – 10^8 molec. cm^{-3}, respectively. And the author mentioned that "An explanation for this could be the very low condensation sink of ~4 × 10^{-4} s^{-1} at Ny-Ålesund…".

Thus, the simulation conditions were set to: T = 268 K, CS = 4.0 × 10^{-4} s^{-1}, [HIO_3] = 10^5 – 10^6, [HIO_2] = 2.0 × 10^3 – 2.0 × 10^4, and [MSA] = 10^6 – 10^8 molec. cm^{-3}.

(b) Marambio: According to the description of Marambio[4], many sunny days are observed, occurring with ambient temperatures above 0 ℃. The author mentioned that the measured gas-phase concentrations of the species of interest showed maxima of ~2.3 × 10^7, and ~3.6 × 10^6 molecules cm^{-3} for the total MSA and HIO_3 concentration, respectively.

Combined with the ranges of [HIO_3] and [MSA] from Figures 5 and 6 in the original paper describing Marambio[4], thus, the simulation conditions were set to: T = 273 K, CS = 1.0 × 10^{-4} s^{-1}, [HIO_3] = 10^5 – 10^6, [HIO_2] = 2.0 × 10^3 – 2.0 × 10^4, and [MSA] = 10^6 – 10^7 molec. cm^{-3}).

(c) Mace Head: In Mace Head, the concentration of HIO_3 during the new particle formation events reached 10^8 molecules cm^{-3}, and the range of [HIO_3] is set to 10^6 – 10^8 molec. cm^{-3} according to Figure 1(b) [5]. Moreover, Berresheim et al. reported that the range of [MSA] is 10^5 – 10^7 molec. cm^{-3}, and the temperature can reach to 14℃, as shown in Figure 6 [6].

Thus, the simulation conditions were set to: T = 287 K, CS = 2.0 × 10^{-3} s^{-1}, [HIO_3] = 10^7 – 10^8, [HIO_2] = 2.0 × 10^5 – 2.0 × 10^6, and [MSA] = 10^6 – 10^7 molec. cm^{-3}.

(d) Réunion: According to Salignat et al., the average [HIO_3] is 2.90 × 10^5 molec. cm^{-3}, and the ranges of [HIO_3] and [MSA] are 10^5 – 10^7 and 10^6 – 10^7 molec. cm^{-3}, respectively, according to Figure 8(a) in the original paper about Réunion [7]. As shown in Figure 4(a), the temperature ranges from 10 to 20 ℃.

Thus, the simulation conditions were set to: T = 288 K, CS = 2.0 × 10^{-3} s^{-1}, [HIO_3] = 10^5 – 3.0 × 10^6, [HIO_2] = 2.0 × 10^3 – 6.0 × 10^4, and [MSA] = 10^6 – 10^8 molec. cm^{-3}.

Item 2) from the reviewer: What's the definition of the *J* in the reported field measurements? Can the reported *J* be directly compared with the ACDC simulated *J*?

Response: In the ACDC simulation, nucleation generally refers to the formation of relatively stable clusters for which collisions with molecules can be assumed to dominate over cluster evaporation. Accordingly, the cluster formation rate (J) indicates the particle flux out of the studied system. In this case, it is the rate of clusters forming at some specific size (*i.e.* the net flux into the size from all other sizes)[1]. In field observation, the formation rates ($J_{1.5}$) were measured by instruments, such as nitrate chemical ionization atmospheric pressure interface Time-Of-Flight mass spectrometer (CI-APi-TOF)[2], differential mobility particle sizer (DMPS) and neutral cluster and air ion spectrometer (NAIS)[4].

According to the Kerminen-Kulmala equation[8], cluster formation rates for d_2 nm clusters (J_{d_2}) relate to those for d_1 nm clusters (J_{d_1}) by

$$J_{d_1} = J_{d_2} \exp\left\{\gamma\left(\frac{1}{d_1} - \frac{1}{d_2}\right)\frac{\mathrm{CS}}{\mathrm{GR}_{d_2\text{-}d_1}}\right\}$$

where the $\mathrm{GR}_{d_2\text{-}d_1}$ is the initial cluster growth rate from d_1 to d_2 nm, and CS represents condensation sink of clusters by preexisting particles. The parameter γ depends on many factors but can usually be approximated by assuming it to be equal to 0.23 nm^2 m^2 h^{-1}.

In this study, the relationship between the formation rates of simulated clusters ($J_{1.2}$) and that of observed clusters ($J_{1.5}$) can be written as:

$$J_{1.2} = J_{1.5} \exp\left\{0.23 \times \left(\frac{1}{1.2} - \frac{1}{1.5}\right)\frac{\mathrm{CS}}{\mathrm{GR}}\right\}$$

where GR was measured to be 3.2 – 4.4 $nm \cdot h^{-1}$ in the 1.1 – 2.0 nm size range during three observed events [9, 10], and CS was 0.002 s^{-1}. $J_{1.2}$ was then calculated to be 1.00001 – 1.00002

times of $J_{1.5}$. Thus, the observed cluster formation rates for 1.5 nm clusters can be directly comparable with the simulated $J_{1.2}$.

We have included corresponding justification in Section 3.4 of the revised manuscript (Lines 242-243, Page 11) and supporting file as follows: "Subsequently, we compared these simulation results with observed nucleation rates and the definition of cluster formation rate was detailed in Supporting Information (SI)."

Item 3) from the reviewer: Moreover, in Line 222, "the observed *J* of 2.1 × 10^{-4} cm^{-3} s^{-1}". This *J* value is too low for a typical NPF event. Is this value obtained from a non-NPF day? Please check the original paper.

Response: Following the reviewer's suggestion, we have carefully checked the original paper. According to the captions of Fig. 2 ("Examples representing seasonal behavior of NPF observed at Villum and Ny-Ålesund")[2], the present *J* of 2.1 × 10^{-4} – 10^{-1} cm^{-3} s^{-1} (Figure 2 (c5)) originate from the observed NPF data values during May 4, 2017. Notably, as professionally judged by the reviewer, Beck et al. have also clarified that data with *J*-values < a few 10^{-3} cm^{-3} s^{-1} (including the mentioned lower *J* of 2.1 × 10^{-4} cm^{-3} s^{-1}) are highly unreliable and reflect mainly the noise levels[2]. And thus, these low and uncertain *J* values hardly correspond to NPF events.

Therefore, we have adjusted the range of the observed *J* of Ny-Ålesund to a reliable range of 10^{-3} – 10^{-1} cm^{-3} s^{-1} in Fig. 6(a). Meanwhile, the related statement "…the *J*(HIO_3-HIO_2-MSA) can be two orders of magnitude higher than the observed *J* of 2.1 × 10^{-4} cm^{-3} s^{-1}" has been changed to "…the *J*(HIO_3-HIO_2-MSA) can be one order of magnitude higher than the observed *J* of 10^{-3} cm^{-3} s^{-1}" in Lines 248-249 (page 11) of the revised manuscript.

Specific comments:

Comment 4: It would be preferable to avoid including reference in the abstract.

Response: The reference in the abstract has been removed in the revised manuscript.

Comment 5: Abbreviations such as ESP HB XB should be explained at least once in the main text.

Response: Thanks for the reviewer's careful reading, all the abbreviations, such as ESP (Electrostatic potential), HB (Hydrogen bond) and XB (Halogen bond), have been explained in their first appearance in the revised manuscript.

Comment 6: Line 47, " Furthermore, given the coexistence of MSA and HIO_3 in different marine regions (Quéléver et al., 2022; Beck et al., 2021), the HIO_3-HIO_2-MSA nucleating mechanism may differ under distinct ambient conditions, but it remains unrevealed." First, nucleating should be nucleation. Second, I feel a bit confusion about this sentence. Is the different HIO_3/MSA and HIO_2/MSA concentration ratio leads to different nucleation mechanism? The authors have concluded that MSA can promote nucleation, particularly in marine regions characterized by lower T, lower [HIO_3] and [HIO_2]. It will be more preferable to add some discussion about the [HIO_3]/ [HIO_2] in different marine atmosphere.

Response: Thanks for the reviewer's helpful comments.

Item 1) from the reviewer: Line 47, " Furthermore, given the coexistence of MSA and HIO_3 in different marine regions (Quéléver et al., 2022; Beck et al., 2021), the HIO_3-HIO_2-MSA nucleating mechanism may differ under distinct ambient conditions, but it remains unrevealed." First, nucleating should be nucleation.

Response: As suggested by the reviewer, all 'nucleating' have been changed to 'nucleation' in the revised manuscript.

Item 2) from the reviewer: Second, I feel a bit confusion about this sentence. Is the different HIO_3/MSA and HIO_2/MSA concentration ratio leads to different nucleation mechanism?

Response: As to the mentioned sentence, in fact, here we would like to express that the dominant nucleation mechanism varies with the region. Accordingly, we have rephrased the sentence (Lines 46-48) as follows: "Furthermore, given the coexistence of MSA and HIO_3 in different marine regions (Quéléver et al., 2022; Beck et al., 2021), along with the consistent presence of HIO_3 and HIO_2 as homologous substances[5], the importance of the HIO_3-HIO_2-MSA nucleation mechanism may differ under distinct ambient conditions, due to their uneven distribution, but it remains unrevealed."

Item 3) from the reviewer: The authors have concluded that MSA can promote nucleation, particularly in marine regions characterized by lower T, lower [HIO_3] and [HIO_2]. It will be more preferable to add some discussion about the [HIO_3]/[HIO_2] in different marine atmosphere.

Response: Furthermore, according to the reviewer's suggestion, we have added the discussion about [HIO_3]/[HIO_2] in the revised manuscript (Lines 224-226, page 10) as follows: "Furthermore, at the conditions with lower [HIO_3]/[HIO_2], where *R* is higher, the contribution of MSA nucleation with HIO_2 increase due to the relative scarcity of HIO_3. Conversely, *R* decreases at higher [HIO_3]/[HIO_2], i.e., the impacts of MSA decreases."

Comment 7: More explanation of ACDC model setting is needed. For example, the setting of condensation sink and other model parameters.

Response: Thanks for reviewer's valuable suggestions. The model parameters in the performed ACDC simulations include: condensation sink (CS), temperature (*T*), precursor concentrations, boundary clusters, collision/evaporation processes (monomer-monomer, monomer-cluster, cluster-cluster). Concerning all the ACDC simulation data presentation, the settings of *T*, CS, and precursor concentrations were provided in the main text and figure captions. And the details on boundary clusters and the employed collision/evaporation processes were added in the Tables S3, S5, and S6 of the Supplementary Information.

Comment 8: Figure 6. The HIO_3-HIO_2 curve should be an area as the other two.

Response: Thanks. The reviewer's comment is important for the clear presentation of the data. Here, we present the rate of HIO_3-HIO_2 nucleation as a line in Fig. 6, due to the setting of the fixed [HIO_3]/[HIO_2] in the simulation, given the homology of HIO_3 and HIO_2, as well as their reported concentration ratio[5]. To avoid potential confusion for readers, we clarified the association between [HIO_3] and [HIO_2] in the caption of Fig. 6, stating: "[HIO_3]/[HIO_2] is a constant".

Comment 9: It would be preferable to include some uncertainty analysis.

Response: Thanks, this is an important point to improve the robustness of the results. The potential uncertainties may arise from ACDC simulations and quantum chemical (QC)

calculations, thereby we examined how variable ACDC settings, such as condensation sink coefficient (CS), sticking factor (SF, corresponding to a sticking probability for cluster/monomer collision) and the change of calculated Gibbs free energy of cluster formation (ΔG, from quantum chemical calculations) impact the enhancement of MSA (R_{MSA}) on cluster formation rate (J). Here, the CS values ranged from 1.0×10^{-4} s^{-1} to 1.0×10^{-2} s^{-1}, covering possible CS in relatively clean and polluted regions[10, 11]. The range of SF was set from 0.1 to 1.0 since sticking probabilities for neutral-neutral collisions between 0.1 and 1.0[12].

As shown in the Figs. S15 (a) and (b), although both CS and SF affect R_{MSA} to some extent, the uncertainty range are relatively limited (CS < 32.5% and SF < 17.1%) and the results does not affect the trend and main conclusions.

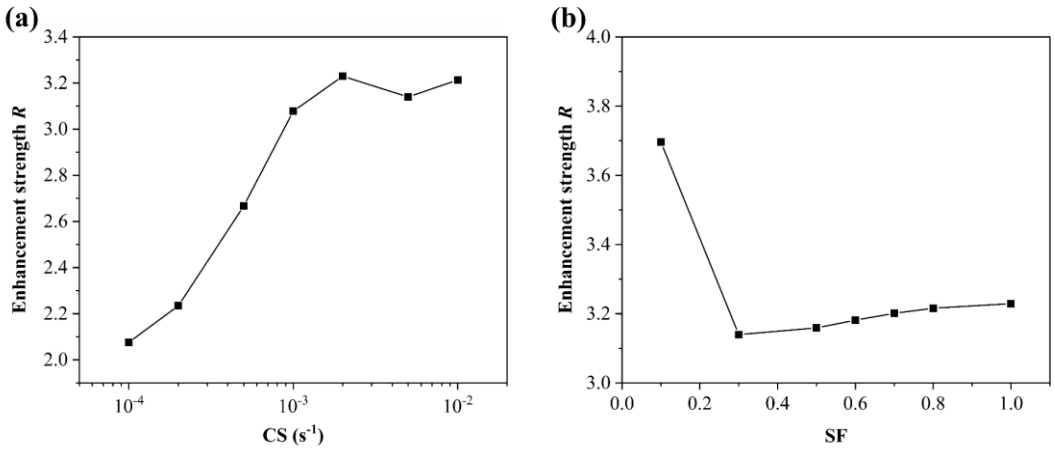

Figure S15. Variation of enhancement strength R of MSA with **(a)** condensation sink coefficient (CS) and **(b)** sticking factor (SF) for HIO_3-HIO_2-MSA system at T = 278 K, [HIO_3] = 1.0×10^7, [HIO_2] = 2.0×10^5, and [MSA] = 1.0×10^7 molec. cm^{-3}.

In addition, the potential uncertainty of quantum chemical calculations is ultimately manifested in the calculated ΔG values. As reported by Kupiainen[13] et al. (2012), the differences between the computational (DFT//RI-CC2 method) and experimental ΔG values are about 1 kcal mol^{-1} or less[14]. Accordingly, Almeida[12] et al. (2013) calculated the uncertainty range of ACDC simulated cluster formation resulting from QC calculations by adjusting the binding energy (±1 kcal mol^{-1}). Further given the consistency of our research framework (DFT//RI-CC2 + ACDC) with Almeida et al. (2013), herein we have performed the uncertainty analysis of R_{MSA} caused by QC calculations through adding or subtracting 1 kcal mol^{-1} from the ΔG (using ΔG_{278K} as a reference). The figure below presents the uncertainty analysis results of

J and R_{MSA} at T = 278 K, CS = 2.0 × 10^{-3} s^{-1}, [HIO_3] = 10^7, [HIO_2] = 2.0 × 10^5, [MSA] = 10^6 – 10^8 molec. cm^{-3}.

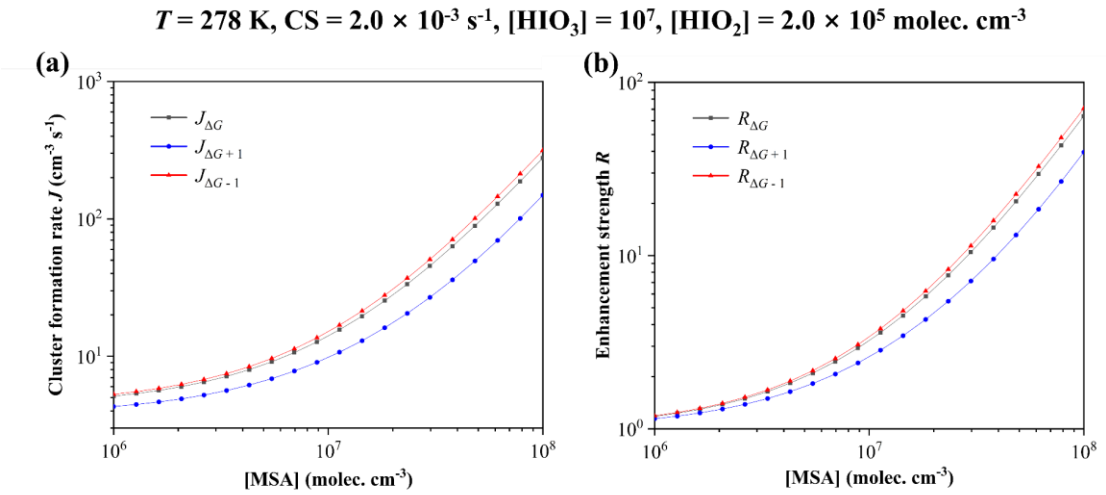

Figure S16. Cluster formation rate J **(a)** and enhancement strength R of MSA **(b)** as a function of [MSA] = 10^6 – 10^8 molec. cm^{-3}, with different energy of ΔG_{278K} (black line), ΔG_{278K} + 1 (blue line), ΔG_{278K} – 1 (red line), at T = 278 K, CS = 2.0 × 10^{-3} s^{-1}, [HIO_3] = 10^7, [HIO_2] = 2.0 × 10^5 molec. cm^{-3}.

Here, we have added the results of R_{MSA} under different CS, SF and ΔG to the revised supporting file, and for the convenience of the review, we have copied Figures S15-S16 and the corresponding analysis as following: "Here, the potential uncertainties may stem from ACDC simulations and quantum chemical (QC) calculations, we examined the effect of condensation sink coefficient (CS), sticking factor (SF) and calculated ΔG of clusters on enhancement of MSA to the cluster formation rate. The CS values ranged from 1.0 × 10^{-4} s^{-1} to 1.0 × 10^{-2} s^{-1}, covering possible CS in relatively clean and polluted regions[10, 11]. The range of SF was set from 0.1 to 1.0 since sticking probabilities for neutral-neutral collisions between 0.1 and 1.0[12]. Both the CS and SF slightly affect the enhancement of MSA, with limited uncertainty range of CS < 32.5% and SF < 17.1% (Fig. S15). As reported by Kupiainen[13] et al. (2012), the differences between the computational (DFT//RI-CC2 method) and experimental ΔG values are about 1 kcal mol^{-1} or less[14]. Accordingly, Almedia[12] et al. (2013) calculated the uncertainty range of ACDC simulated cluster formation resulting from QC calculations by adjusting the binding energy (±1 kcal mol^{-1}). Further given the consistency of our research framework (DFT//RI-CC2 + ACDC) with Almedia et al. (2013), herein we have performed the

uncertainty analysis of R_{MSA} caused by QC calculations through adding or subtracting 1 kcal mol^{-1} from the ΔG (using ΔG_{278K} as a reference). As shown in Table S8 and Fig. S16, adjusting the ΔG_{278K} of clusters by ±1 kcal mol^{-1} resulted in a minor variation in J and R of MSA, with the overall trend remaining consistent."

Reference:

[1] K.-M. Oona, O. Tinja, Atmospheric Cluster Dynamics Code Technical manual, https://github.com/tolenius/ACDC/blob/main/ACDC_Manual_2020_11_25.pdf (2020).

[2] L.J. Beck, N. Sarnela, H. Junninen, C.J.M. Hoppe, O. Garmash, F. Bianchi, M. Riva, C. Rose, O. Peräkylä, D. Wimmer, O. Kausiala, T. Jokinen, L. Ahonen, J. Mikkilä, J. Hakala, X.C. He, J. Kontkanen, K.K.E. Wolf, D. Cappelletti, M. Mazzola, R. Traversi, C. Petroselli, A.P. Viola, V. Vitale, R. Lange, A. Massling, J.K. Nøjgaard, R. Krejci, L. Karlsson, P. Zieger, S. Jang, K. Lee, V. Vakkari, J. Lampilahti, R.C. Thakur, K. Leino, J. Kangasluoma, E.M. Duplissy, E. Siivola, M. Marbouti, Y.J. Tham, A. Saiz-Lopez, T. Petäjä, M. Ehn, D.R. Worsnop, H. Skov, M. Kulmala, V.M. Kerminen, M. Sipilä, Differing Mechanisms of New Particle Formation at Two Arctic Sites, Geophys. Res. Lett. 48 (2021).

[3] NASA POWER. Data access viewer. https://power.larc.nasa.gov/data-accessviewer/, (2022).

[4] L.L.J. Quéléver, L. Dada, E. Asmi, J. Lampilahti, T. Chan, J.E. Ferrara, G.E. Copes, G. Pérez-Fogwill, L. Barreira, M. Aurela, D.R. Worsnop, T. Jokinen, M. Sipilä, Investigation of new particle formation mechanisms and aerosol processes at Marambio Station, Antarctic Peninsula, Atmos. Chem. Phys. 22 (2022) 8417–8437.

[5] M. Sipilä, N. Sarnela, T. Jokinen, H. Henschel, H. Junninen, J. Kontkanen, S. Richters, J. Kangasluoma, A. Franchin, O. peräkylä, M.P. Rissanen, M. Ehn, H. Vehkamäki, T. Kurten, T. Berndt, T. Petäjä, D. Worsnop, D. Ceburnis, V.M. Kerminen, M. Kulmala, C. O'Dowd, Molecular-scale evidence of aerosol particle formation via sequential addition of HIO_3, Nature 537 (2016) 532–534.

[6] H. Berresheim, T. Elste, K. Rosman, M. Dal Maso, H.G. Tremmel, J.M. Mäkelä, A.G. Allen, M. Kulmala, H.-C. Hansson, Gas-aerosol relationships of H_2SO_4, MSA, and OH: Observations in the coastal marine boundary layer at Mace Head, Ireland, J. Geophys. Res.-Atmos. 107 (2002) PAR 5-1–PAR 5-12.

[7] R. Salignat, M. Rissanen, S. Iyer, J.-L. Baray, P. Tulet, J.-M. Metzger, J. Brioude, K. Sellegri, C. Rose, Measurement Report: Insights into the chemical composition of molecular clusters present in the free troposphere over the Southern Indian Ocean: observations from the Maïdo observatory (2150 m a.s.l., Reunion Island), EGUsphere (2023) 1–41.

[8] M. Kulmala, T. Petäjä, T. Nieminen, M. Sipilä, H.E. Manninen, K. Lehtipalo, M. Dal Maso, P.P. Aalto, H. Junninen, P. Paasonen, I. Riipinen, K.E.J. Lehtinen, A. Laaksonen, V.-M. Kerminen, Measurement of the nucleation of atmospheric aerosol particles, Nature Protocols 7 (2012) 1651-1667.

[9] D. Xia, J. Chen, H. Yu, H.B. Xie, Y. Wang, Z. Wang, T. Xu, D.T. Allen, Formation Mechanisms of Iodine-Ammonia Clusters in Polluted Coastal Areas Unveiled by Thermodynamics and Kinetic Simulations, Environ. Sci. Technol. 54 (2020) 9235-9242.

[10] H. Yu, L. Ren, X. Huang, M. Xie, J. He, H. Xiao, Iodine speciation and size distribution in ambient aerosols at a coastal new particle formation hotspot in China, Atmos. Chem. Phys. 19 (2019) 4025–4039.

[11] X.-C. He, Y.J. Tham, L. Dada, M. Wang, H. Finkenzeller, D. Stolzenburg, S. Iyer, M. Simon, A.K. ¨rten, J. Shen, B. Roerup, M. Rissanen, S. Schobesberger, R. Baalbaki, D.S. Wang, T.K. Koenig, T. Jokinen, N. Sarnela, L.J. Beck, J. Almeida, S. Amanatidis, A. Amorim, F. Ataei, A. Baccarini, B. Bertozzi, F. Bianchi, S. Brilke, L. Caudillo, D. Chen, R. Chiu, B. Chu, A. Dias, A. Ding, J. Dommen, J. Duplissy, I.E. Haddad, L.G. Carracedo, M. Granzin, A. Hansel, M. Heinritzi, V. Hofbauer, H. Junninen, J. Kangasluoma, D. Kemppainen, C. Kim, W. Kong, J.E. Krechmer, A. Kvashin, T. Laitinen, H. Lamkaddam, C.P. Lee, K. Lehtipalo, M. Leiminger, Z. Li, V. Makhmutov, H.E. Manninen, G. Marie, R. Marten, S. Mathot, R.L. Mauldin, B. Mentler, O. Moehler, T. Mueller, W. Nie, A. Onnela, T. Petaja, J. Pfeifer, M. Philippov, A. Ranjithkumar, A. Saiz-Lopez, I. Salma, W. Scholz, S. Schuchmann, B. Schulze, G. Steiner, Y. Stozhkov, C. Tauber, A. Tome, R.C. Thakur, O. Vaisanen, M. Vazquez-Pufleau, A.C.

Wagner, Y. Wang, S.K. Weber, P.M. Winkler, Y. Wu, M. Xiao, C. Yan, Q. Ye, A. Ylisirnio, M. Zauner-Wieczorek, Q. Zha, P. Zhou, R.C. Flagan, J. Curtius, U. Baltensperger, M. Kulmala, V.-M. Kerminen, T. Kurten, N.M. Donahue, R. Volkamer, J. Kirkby, D.R. Worsnop, M. Sipila, Role of iodine oxoacids in atmospheric aerosol nucleation, Science 371 (2021) 589–595.

[12] J. Almeida, S. Schobesberger, A. Kürten, I.K. Ortega, O. Kupiainen-Määttä, A.P. Praplan, A. Adamov, A. Amorim, F. Bianchi, M. Breitenlechner, A. David, J. Dommen, N.M. Donahue, A. Downard, E. Dunne, J. Duplissy, S. Ehrhart, R.C. Flagan, A. Franchin, R. Guida, J. Hakala, A. Hansel, M. Heinritzi, H. Henschel, T. Jokinen, H. Junninen, M. Kajos, J. Kangasluoma, H. Keskinen, A. Kupc, T. Kurten, A.N. Kvashin, A. Laaksonen, K. Lehtipalo, M. Leiminger, J. Leppä, V. Loukonen, V. Makhmutov, S. Mathot, M.J. McGrath, T. Nieminen, T. Olenius, A. Onnela, T. Petäjä, F. Riccobono, I. Riipinen, M. Rissanen, L. Rondo, T. Ruuskanen, F.D. Santos, N. Sarnela, S. Schallhart, R. Schnitzhofer, J.H. Seinfeld, M. Simon, M. Sipilä, Y. Stozhkov, F. Stratmann, A. Tomé, J. Tröstl, G. Tsagkogeorgas, P. Vaattovaara, Y. Viisanen, A. Virtanen, A. Vrtala, P.E. Wagner, E. Weingartner, H. Wex, C. Williamson, D. Wimmer, P. Ye, T. Yli-Juuti, K.S. Carslaw, M. Kulmala, J. Curtius, U. Baltensperger, D.R. Worsnop, H. Vehkamäki, J. Kirkby, Molecular understanding of sulphuric acid-amine particle nucleation in the atmosphere, Nature 502 (2013) 359–363.

[13] O. Kupiainen, I.K. Ortega, T. Kurtén, H. Vehkamäki, Amine substitution into sulfuric acid – ammonia clusters, Atmos. Chem. Phys. 12 (2012) 3591-3599.

[14] K.D. Froyd, E.R. Lovejoy, Bond energies and structures of ammonia-sulfuric acid positive cluster ions, J. Phys. Chem. A 116 (2012) 5886-5899.